

Polarizabilities as a test of localized approximations to the self-interaction correction

J. Messud^{a,b,*}, Z. Wang^{a,b,c}, P. M. Dinh^{a,b},
P.-G. Reinhard^d and E. Suraud^{a,b}

^a *Université de Toulouse; UPS;
Laboratoire de Physique Théorique (IRSAMC); F-31062 Toulouse, France*

^b *CNRS; LPT (IRSAMC); F-31062 Toulouse, France*

^c *Institute of Low energy Nuclear Physics, Beijing Normal University, Beijing
100875, China*

^d *Institut für Theoretische Physik, Universität Erlangen, D-91058 Erlangen,
Germany*

Abstract

We present applications of the recently introduced “Generalized SIC-Slater” scheme which provides a simple Self-Interaction Correction approximation in the framework of the Optimized Effective Potential. We focus on the computation of static polarizabilities which are known to constitute stringent tests for Density Functional Theory. We apply the new method to model H chains, but also to more realistic systems such as C₄ (organic) chains, and less symmetrical systems such as a Na₅ (metallic) cluster. Comparison is made with other SIC schemes, especially with the standard SIC-Slater one.

Key words: Density Functional Theory, Self-Interaction Correction, Optimized Effective Potential, SIC-Slater approximation, Static polarizability

PACS: 71.15.Mb, 31.15.E-, 73.22.-f, 31.15.ap

1 Introduction

Density-functional theory (DFT) has become over the years one of the most

* Corresponding author

Email-address : messud@irsamc.ups-tlse.fr

powerful theories for the description of complex electronic systems ranging from atoms and molecules, to bulk solids. It allows realistic calculations of an ever increasing number of systems in physics and chemistry [1,2,3]. As the exact functional is not known, most applications employ the Local Density Approximation (LDA), see e.g. [4], or its extension to the Generalized Gradient Approximation (GGA) [5]. In spite of their successes, these approaches still have deficiencies. In particular, the self-interaction error spoils single-particle properties as, e.g., the ionization potential [6,7]. Another critical detail where LDA and GGA usually fail is the polarizability in chain molecules [8,9]. An intuitive and efficient solution is to augment LDA by a Self-Interaction Correction (SIC) [10,11], i.e. to introduce an explicit orbital dependence of the functional by subtracting by hand the spurious self-interaction. The drawback is that it produces a state-dependent mean-field Hamiltonian which requires extra efforts to enforce orthogonality of the single particle basis [11,12,13,14]. The optimized effective potential (OEP) method [15,16,17,18] overcomes that complication as it allows to define the best common (state-independent) local mean-field potential $V(\mathbf{r})$. Indeed some crucial features of the underlying SIC as, e.g., the localization of states or the derivative discontinuity [19,20] are found to be maintained through an OEP procedure [21], for a comprehensive overview see [15]. But the exhaustive SIC-OEP equations are difficult to handle and are thus often simplified. A most popular approximation is the so-called Krieger-Li-Iafrate (SIC-KLI) approach [16,17] and, in a further step of simplification, the SIC-Slater approximation [22]. However, SIC-KLI and SIC-Slater approximations can easily miss crucial features of SIC as, e.g., the performance with respect to polarizability, even if accurate exchange-correlation potentials are used [23] (note that the same conclusion holds at the exact-exchange level [9]).

A key question is the localization of orbitals, as had been already observed rather early [24], which then minimizes the electronic interaction energy. Indeed states which optimize SIC tend to be localized whereas states emerging from a common local mean-field tend to more delocalization. These contradicting demands can be bridged by full OEP but spoil approximate treatments as SIC-KLI or SIC-Slater approximation. A fairly convenient way out is to use two sets of orbitals. That was already proposed in [25] and has been used to improve on the SIC-KLI approximation [26,27,28], although not yet in a fully consistent and variational form. Taking up the double-set idea, we have recently proposed a SIC-OEP scheme relying on two sets of complementing orbitals [29]. At the purely stationary full SIC level, it is mostly a matter of convenience, while a double-set technique becomes crucial in practical applications of the time-dependent SIC [14]. In this paper, we will also demonstrate that this method can be powerfully exploited in stationary calculations in the frame of SIC-OEP. Indeed the two sets are connected by a unitary transformation, thus building the same total density. One of the sets remains spatially localized while the other set is free to accommodate a common local potential

and/or minimal energy variance. The spatially localized set is determined by variation of the SIC energy with respect to unitary transformation coefficients which allows that these states fulfill what is called the “symmetry condition” [14,25,29,30]. The localized set shows a much better performance with respect to standard SIC-KLI or SIC-Slater approximation. The resulting formalism is called “Generalized SIC-OEP” [29]. We further simplified the resulting equations, following the track of the SIC-Slater approximation and developed in a strictly variational manner a double-set treatment of the SIC-Slater approximation to OEP, namely the “Generalized SIC-Slater” approximation. It is to be noted that a very similar development is found in [31]. As one of the sets remains spatially localized, it validates the Generalized SIC-Slater approximation to Generalized SIC-OEP built from this set, while maintaining key features of the full SIC scheme: it is energetically advantageous for the SIC energy, permits to re-establish potential energy surfaces (PES), and performs fairly well in the calculations of polarizabilities. We pointed out that the Generalized SIC-Slater emerges naturally because of the localization of one set of orbitals [29], whereas Körzdörfer *et al.* [31] compared Generalized SIC-KLI and full Generalized SIC-OEP with standard SIC-KLI and OEP and also with the approximate Generalized SIC-KLI of [28]. It is to be noted that the practical introduction of localized orbitals within the SIC-KLI approximation has also been proposed in [26,27,28] without explicit “symmetry condition”. The form of the SIC-KLI approximation used in those papers is not exactly what comes out from the more fundamental “Generalized SIC-OEP” [31]. After a brief presentation of the formalism, we apply it to model hydrogen chains, and to various other systems such as C (organic) chains and Na (metallic) clusters.

2 The Generalized SIC-Slater formalism

2.1 Summary of SIC equations

We briefly summarize the formalism using for simplicity a notation without explicit spin densities. The generalization to these is obvious. The calculations later on use, of course, the full spin density functional.

The starting point for the formulation of SIC is the SIC energy functional for electrons

$$E_{\text{SIC}} = E_{\text{kin}} + E_{\text{ion}} + E_{\text{LDA}}[\rho] - \sum_{\beta=1}^N E_{\text{LDA}}[\rho_{\beta}], \quad \rho = \sum_{\beta=1}^N \rho_{\beta}, \quad \rho_{\beta} = |\psi_{\beta}|^2 \quad (1)$$

where $E_{\text{LDA}}[\rho]$ is a standard LDA energy-density functional (which contains

both the Hartree and the exchange-correlation energies in our notations) complementing the kinetic energy E_{kin} and the interaction energy with the ionic background E_{ion} . The last term is the SIC correction. The densities ρ_α and ρ are defined from the set of occupied single-particle states $\{\psi_\beta, \beta = 1 \dots N\}$. The SIC equations are obtained by standard variational techniques within imposing explicit orthonormalization of the orbitals by a set of Lagrange multipliers $\lambda_{\alpha\beta}$. We now introduce a second set of orbitals $\{\varphi_i\}$ related to the previous one by a unitary transformation within the set of occupied states (i.e. leading to the same total density $\rho : \varphi_i = \sum_\alpha u_{i\alpha}^* \psi_\alpha$) which diagonalizes the $\lambda_{\alpha\beta}$. We can then recast the resulting equations in eigenvalue equations [25,29,30]

$$\hat{h}_{\text{SIC}}|\varphi_i\rangle = \varepsilon_i|\varphi_i\rangle \quad (2)$$

$$0 = (\psi_\beta|U_\beta - U_\alpha|\psi_\alpha) \quad (3)$$

with the SIC Hamiltonian reading

$$\hat{h}_{\text{SIC}} = \hat{h}_{\text{LDA}} - \sum_\alpha U_\alpha |\psi_\alpha\rangle \langle \psi_\alpha| \quad (4a)$$

$$\hat{h}_{\text{LDA}} = \frac{\hat{p}^2}{2m} + U_{\text{LDA}}[\rho](\mathbf{r}), \quad \text{with} \quad U_{\text{LDA}}[\rho](\mathbf{r}) = \frac{\delta E_{\text{LDA}}[\rho]}{\delta \rho(\mathbf{r})} \quad (4b)$$

$$U_\alpha(\mathbf{r}) = \frac{\delta E_{\text{LDA}}[\rho_\alpha]}{\delta \rho_\alpha(\mathbf{r})} = U_{\text{LDA}}[|\psi_\alpha|^2](\mathbf{r}) \quad (4c)$$

where \hat{h}_{LDA} is the standard LDA Hamiltonian. The coefficients $u_{i\alpha}$ of the unitary transformation for given *diagonal* orbitals φ_i are determined such that the ψ_α satisfy the symmetry condition (3). The ψ_α are called *localized* orbitals because they are spatially much more localized [25,30].

2.2 SIC and OEP

The eigenvalue equation (2) employs a non-local Hamiltonian \hat{h}_{SIC} , see Eq. (4a), which complicates the numerical handling. In [29], we proposed to apply the OEP formalism to this two-sets SIC formulation, to find the best local approximation to its Hamiltonian. A very similar development is found in [31]. We start from a set φ_i which satisfies the eigenvalue equations (this set is not exactly the same as that of the exact SIC equation because additional restriction of the Hilbert space is imposed here – this point being clarified, we will employ the same symbol to simplify the notations) :

$$\left[\hat{h}_{\text{LDA}}(\mathbf{r}) - V_0(\mathbf{r}) \right] \varphi_i(\mathbf{r}) = \varepsilon_i \varphi_i(\mathbf{r}) \quad , \quad (5)$$

where V_0 is a local and state-independent potential which needs to be optimized to minimize the SIC energy (1). It is important to note that this energy is still expressed in terms of the ψ_α , linked by a unitary transformation to the φ_i and which satisfy the symmetry condition (3) in our case. The optimized effective potential $V_0(\mathbf{r})$ is found by variation $\delta E_{\text{SIC}}/\delta V_0(\mathbf{r}) = 0$. We obtain $V_0 = V_S + V_K + V_C$, with [29,31]

$$V_S = \sum_{\alpha} \frac{|\psi_{\alpha}|^2}{\rho} U_{\text{LDA}}[|\psi_{\alpha}|^2] \quad , \quad (6a)$$

$$V_K = \frac{1}{\rho} \sum_{\alpha, \beta} \left(\sum_i |\varphi_i|^2 v_{i\alpha}^* v_{i\beta} \right) (\psi_{\beta} | V_0 - U_{\text{LDA}}[|\psi_{\alpha}|^2] | \psi_{\alpha}) \quad , \quad (6b)$$

$$V_C = \frac{1}{2} \sum_i \frac{\nabla \cdot (p_i \nabla |\varphi_i|^2)}{\rho} \quad , \quad (6c)$$

$$p_i(\mathbf{r}) = \frac{1}{\varphi_i^*(\mathbf{r})} \sum_{\alpha} v_{i\alpha} \int d\mathbf{r}' \left(V_0(\mathbf{r}') - U_{\text{LDA}}[|\psi_{\alpha}|^2](\mathbf{r}') \right) \psi_{\alpha}^*(\mathbf{r}') G_i(\mathbf{r}, \mathbf{r}') \quad , \quad (6d)$$

$$G_i(\mathbf{r}, \mathbf{r}') = \sum_{j \neq i} \frac{\varphi_j^*(\mathbf{r}) \varphi_j(\mathbf{r}')}{\varepsilon_j - \varepsilon_i} \quad . \quad (6e)$$

2.3 Generalized SIC-Slater

The involved OEP equations can be simplified by exploiting the property that the ψ_{α} are spatially localized [25], which yields $V_0|\psi_{\alpha} \rangle \approx U_{\text{LDA}}[|\psi_{\alpha}|^2]|\psi_{\alpha} \rangle$. This allows to employ the SIC-Slater approximation to OEP, yielding [29] :

$$V_0(\mathbf{r}) \simeq \sum_{\alpha} \frac{|\psi_{\alpha}(\mathbf{r})|^2}{\rho(\mathbf{r})} U_{\text{LDA}}[|\psi_{\alpha}|^2](\mathbf{r}) \quad , \quad (7)$$

Note that this equation has the form of a SIC-Slater approximation [21,32] but is constructed from the localized orbitals ψ_{α} and is applied to the diagonal orbitals φ_i . We called this new scheme ‘‘Generalized SIC-Slater’’ (GSlat) approximation, which differs from the standard SIC-Slater scheme because of the two basis sets involved here and which, therefore, has more flexibility. The practical scheme for GSlat can be summarized as follows : *i*) Eq. (5) generates the ‘‘diagonal’’ set φ_i of occupied states; *ii*) the unitary transformation serves to accommodate the symmetry condition (3) which, in turn, defines the ‘‘localized’’ set ψ_{α} ; *iii*) the latter set enters the OEP V_0 as given in Eq. (7).

2.4 Generalized SIC-KLI and approximations thereof

Even if the GSlat approximation might be satisfying in most cases, it is worth discussing in more detail the SIC-KLI correction (6b). The use of the localization of the ψ_α allows to keep only the diagonal terms $\alpha = \beta$, that is,

$$V_K \approx \frac{1}{\rho} \sum_\alpha \left(\sum_i |v_{i\alpha}^* \varphi_i|^2 \right) (\psi_\alpha | V_0 - U_{\text{LDA}}[|\psi_\alpha|^2] | \psi_\alpha). \quad (8)$$

In contrast to the GSlat approximation, fluctuations of $V_0|\psi_\alpha\rangle$ around $U_{\text{LDA}}[|\psi_\alpha|^2]|\psi_\alpha\rangle$ are not neglected, even if one expects them to remain small.

It is now instructive to use the following identity :

$$\left| \sum_i v_{i\alpha}^* \varphi_i \right|^2 = \sum_i |v_{i\alpha}^* \varphi_i|^2 + \sum_{\substack{i,j \\ i \neq j}} (v_{i\alpha}^* \varphi_i)(v_{j\alpha}^* \varphi_j)^*,$$

to multiply it by $(\psi_\alpha | V_0 - U_{\text{LDA}}[|\psi_\alpha|^2] | \psi_\alpha)$ and to sum over α . We thus obtain :

$$\sum_\alpha |\psi_\alpha|^2 (\psi_\alpha | V_0 - U_{\text{LDA}}[|\psi_\alpha|^2] | \psi_\alpha) = \sum_i A_{ii} + \sum_{\substack{i,j \\ i \neq j}} A_{ij} \quad , \quad (9a)$$

where

$$A_{ij} = \varphi_i \varphi_j^* \sum_\alpha v_{i\alpha}^* v_{j\alpha} (\psi_\alpha | V_0 - U_{\text{LDA}}[|\psi_\alpha|^2] | \psi_\alpha). \quad (10)$$

First, we have the expression $V_K \approx \frac{1}{\rho} \sum_i A_{ii}$ where we used the approximate form (8) of the SIC-KLI correction. If one further assumes that for $i \neq j$, $|A_{ij}| \ll |A_{ii}|$, one obtains the following approximation of the SIC-KLI correction

$$V_K \approx \frac{1}{\rho} \sum_\alpha |\psi_\alpha|^2 (\psi_\alpha | V_0 - U_{\text{LDA}}[|\psi_\alpha|^2] | \psi_\alpha) \quad , \quad (11)$$

which is the form proposed in [26,27,28] without reference to the symmetry condition. This expression can thus be derived from an approximation of the so-called ‘‘Generalized SIC-KLI’’ potential. We will call it ‘‘Localized SIC-KLI’’ (Loc. SIC-KLI) thereafter.

The justification of the approximation $|A_{ij}| \ll |A_{ii}|$ remains to be clarified. A way to circumvent the formal difficulty is to consider practical applications to see how the approximation performs. Still, the assumption probably holds for spatially symmetric systems, as will be discussed lengthly when tested on hydrogen chains (see Sec. 3.1). The case of asymmetrical systems however remains to be explored in more detail, especially in comparison to the formally better founded forms (6b) or (8).

2.5 Summary

All SIC mean-field Hamiltonians presented above enter a Schrödinger-like equation of the form $\hat{h}|\varphi_i\rangle = \epsilon_i|\varphi_i\rangle$. We have thus summarized them in table 1, so that one can easily track the various contributions from one Hamiltonian to another. Note that the symmetry condition (3) should be added for the last

Expression of \hat{h} in $\hat{h} \varphi_i\rangle = \epsilon_i \varphi_i\rangle$	Method
$\hat{h}_{\text{LDA}}[\rho]$	LDA
$\hat{h}_{\text{LDA}}[\rho] - \hat{U}_{\text{LDA}}\left[\frac{\rho}{N}\right]$	Average Density SIC
$\hat{h}_{\text{LDA}}[\rho] - \sum_j \frac{ \varphi_j ^2}{\rho} \hat{U}_{\text{LDA}}[\varphi_j ^2]$	Standard SIC-Slater
$\hat{h}_{\text{LDA}}[\rho] - \sum_\alpha \frac{ \psi_\alpha ^2}{\rho} \hat{U}_{\text{LDA}}[\psi_\alpha ^2]$	Generalized SIC-Slater
$\hat{h}_{\text{LDA}}[\rho] - \sum_\alpha \frac{ \psi_\alpha ^2}{\rho} \hat{U}_{\text{LDA}}[\psi_\alpha ^2] - \frac{1}{\rho} \sum_\alpha \psi_\alpha ^2 (\psi_\alpha V_0 - U_{\text{LDA}}[\psi_\alpha ^2] \psi_\alpha)$	Localized SIC-KLI
$\hat{h}_{\text{LDA}}[\rho] - \sum_\alpha \hat{U}_{\text{LDA}}[\psi_\alpha ^2] \psi_\alpha\rangle \langle \psi_\alpha $	Exact SIC (benchmark)

Table 1

The hierarchy of mean-field Hamiltonians, from simple-most LDA (top line) to full SIC (bottom line), called “exact” SIC.

three schemes, to define the localized states ψ_α required in the corresponding Hamiltonians.

2.6 Computational details

The test cases presented in this paper have been obtained using a full 3D DFT code originally developed for large scale calculations of the dynamics of metal clusters [33] and later on small hydrogen clusters [34], and now extended to treat any organic system [35]. The electronic wave functions are represented on an equidistant 3D grid with fixed mesh size (between 0.4 and 0.8 a_0 , depending on the studied system). The ionic background is treated by means of pseudopotentials, using either local ones (Na, H) [36] or non-local ones to treat organic systems [37]. Even in the case of hydrogen, we use a pseudopotential in order to regularize the Coulomb singularity at origin (the Giannozzi pseudopotential as in [23]). The pseudopotential parameters, especially the core size, fixes the optimal grid representation. For the molecular chains calculations, we use boxes of 40 – 52 a_0 in the longitudinal direction (according to the case) and 20 a_0 in the transverse directions. For the Na₅ cluster, we use a box

of $38 a_0$ in each direction. Those sizes are sufficiently large to provide good convergence properties of calculations. For completeness, computations have been checked using larger boxes with no noticeable differences in the results. Electronic ground states are obtained by damped gradient iterations.

3 Static polarizability results

We had shown in [29] that GSlater solves the problem with potential-energy surfaces encountered in the standard SIC-Slater scheme and produces good results for the polarizability of the C atom. Here we will show through full 3D calculations that it also yields favorable results for more complex structures: model H chains, C_4 chains and a Na_5 cluster. We compare the GSlater results to LDA, ADSIC (Average Density SIC) [38], standard SIC-Slater and exact SIC results, the latter being the benchmark. For the comparison, we use the static dipole polarizability as a most sensitive test for DFT approximations [39]. Considering a system put inside an electrical field \mathbf{E} , the polarizability is defined as $\alpha_i = \partial\mu_i/\partial E_i$, where μ_i is the dipole moment along the i direction and E_i the electric field along i .

3.1 Hydrogen chains

Linear chains of H atoms constitute (highly) simplified model systems for various important chain or chain-like molecules such as in particular polyacetylene with its remarkable properties [40]. These model systems are of great interest to investigate DFT schemes [23,41] as they are particularly difficult to be correctly described within LDA [27]. They thus provide a critical test.

Our calculations on polarizabilities in hydrogen chains are presented in Fig. 1 and are compared with previous results [28,23,42]. For sake of a fair comparison, we have taken care of using the same pseudopotential as used in former calculations because we found that using different pseudopotentials leads to different absolute values of the highly sensitive polarizabilities. This point may look surprising especially in the case of hydrogen for which inserting a pseudopotential is a matter of practical convenience for regularizing grid representations. However, as the grid size is optimized to the regularizing core, different core widths lead to slightly different finite representations of the wave functions (having of course the same energy). This may deliver slightly different values of polarizabilities. This has to be kept in mind when comparing with MP4 results which are computed in a different fashion. But the comparison between the various DFT approaches stays on safe grounds.

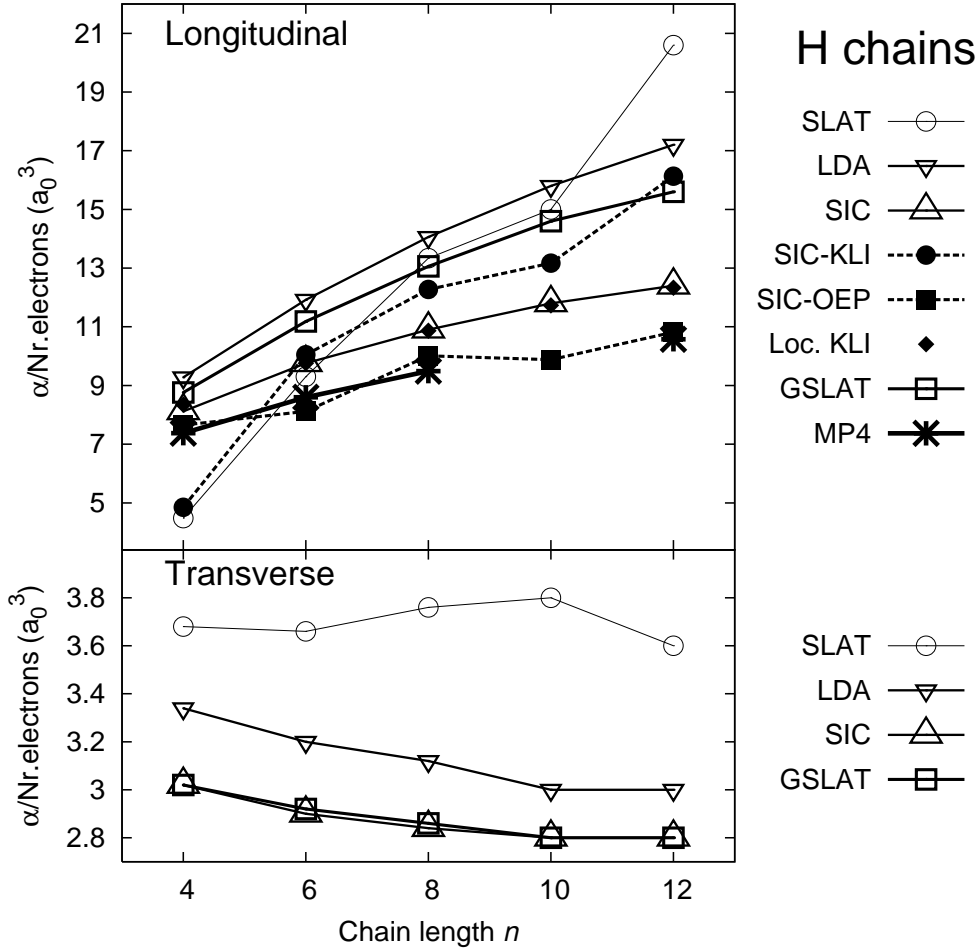


Fig. 1. Top : Longitudinal polarizabilities of H_n chains (per hydrogen atom, in a_0^3) as a function of length n , for an alternation of 2 and 3 a_0 bond length in various calculations; we present our own LDA, SIC, standard SIC-Slater and GSlat results (open symbols) in comparison with calculations from other groups: standard SIC-KLI [23], standard SIC-OEP [23], Loc. SIC-KLI [28] and quantum chemistry MP4 [42]. Bottom: Transverse polarizabilities of H chains (our own results only).

We first mention that our LDA and SIC calculations perfectly match previously published results [43] (not shown in the figure). Furthermore the trends are rather systematic: LDA strongly overestimates polarizabilities, as expected, and SIC comes much closer to MP4 results. Still the most relevant comparison, in our opinion, is that between SIC and approximations thereof, because of the pseudopotential effects mentioned above.

There are several interesting points showing up from this comparison. First, while standard SIC-Slater (open circles) and standard SIC-KLI (full circles) calculations lead to results of varying quality, we see that GSlat (open squares), even if not perfectly matching exact SIC, leads to overall acceptable results showing more regular and realistic trends. However the agreement in absolute

values tends to degrade with increasing chain length, in relative values (of GSlat compared to SIC) : from +8% to +25% from H_4 to H_{12} . Hence one can wonder whether less dramatic approximations to the Generalized SIC-OEP formalism would improve the results. An obvious next step is to use the Generalized SIC-KLI correction instead of GSlat. We show in Fig. 1 the Loc. SIC-KLI results obtained by [28] with the addition of the approximate Generalized SIC-KLI term as given in Eq. (11). Mind that these results used another localization criterion than the symmetry condition. As seen in the figure, perfect agreement with SIC is achieved (compare large open triangles with black diamonds). This thus validates *a posteriori* the assumption done to obtain (11). We however recall that Eq. (11) has no robust foundation. The Loc. SIC-KLI results nevertheless demonstrate the promising possibility to use a numerically less costly localization criterion than the symmetry condition. Indeed, the equivalent GSlat in [28] perfectly agrees with ours.

The mechanism invoked to explain the better performance of SIC-KLI (standard and generalized) on polarizabilities, over mere LDA or standard SIC-Slater, is that the SIC-KLI correction, or the so-called response part of the exchange-correlation potential defined in [8], produces a counter-field effect [8] : with an external field, the exchange-correlation potential behaves globally against it. Electronic motion is hindered and polarizabilities are thus reduced compared with a LDA treatment. The counter-field effect is all the more efficient when one goes from SIC-KLI to OEP [41,23] or in a Generalized SIC-KLI treatment [28]. In GSlat, no response potential is present, so no counter-field effect is expected here. Indeed, the average GSlat exchange-correlation potential in the presence of an external field is not opposite to the electric potential, as the SIC-KLI or the OEP ones are (see e.g. bottom panels of Fig. 2 in [28] which correspond to our GSlat but obtained with another localization criterion than the symmetry condition). Actually, the performance of our GSlat approximation stands in the property that much higher barriers (than in standard SIC-Slater or SIC-KLI) between H_2 units appear in the exchange-correlation potential, which hinder more the electronic motion. This has to be linked to the localized character of the orbitals that enter into its calculation [28].

It would be extremely interesting to also test the Generalized SIC-KLI and its various approximate forms in less symmetrical systems. This calls for a systematic study which will be reported in a forthcoming paper. Keeping this in mind, we will nevertheless present in the following a few examples of applications to less symmetrical systems in the case of GSlat in comparison to exact SIC.

Before doing so, let us remark that the case of full standard OEP results of [23] (close squares) deserve a special comment. Indeed, up to fluctuations, the obtained results perfectly match the MP4 ones (stars), and thus somewhat differ from SIC ones. There is here a matter of interpretation in the sense that,

if the aim is to match MP4 results, the results are perfect. But if it is to find a good approximation to SIC then the agreement is not dramatically better than GSlat ones (relative values of OEP compared to SIC : -6% to -13% from H_4 to H_{12}) and is worse than the Loc. SIC-KLI ones. Moreover GSlat and Loc. SIC-KLI calculations seen as approximations to full Generalized SIC-OEP are cheaper schemes, easily applicable to much more complex systems than hydrogen chains.

Note finally that Fig. 1 also shows the transverse polarizability for those hydrogen chains. In that case, the GSlat approximation reproduces perfectly the exact SIC results, as expected.

Now that the capability of GSlat on hydrogen chains has been checked, we deeper analyze the properties of the system in a small chain, namely H_4 . We

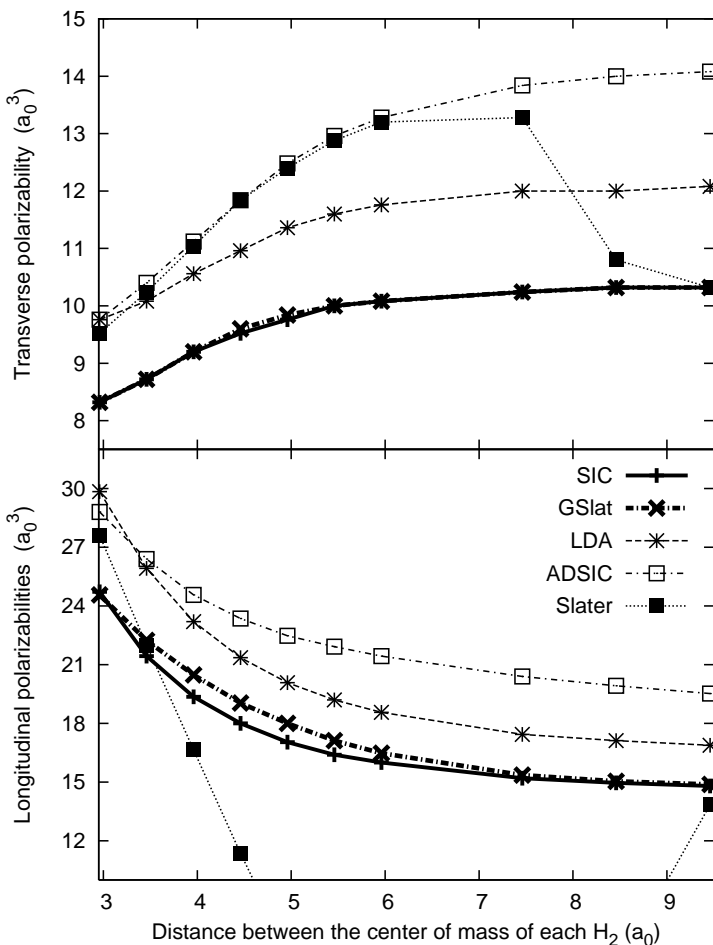


Fig. 2. Longitudinal (top) and tranverse (bottom) polarizabilities of H_4 chains, according to the H_2 - H_2 center of mass distance, for various SIC schemes as indicated.

present in Fig. 2 the values of the (longitudinal and transverse) polarizabilities of H_4 chains, according to various H_2 - H_2 center of mass distances. Here

we used the experimental value of the H_2 bond length, that is $1.46 a_0$. The data labeled “SIC” constitutes our benchmark. LDA (stars) overestimates polarizabilities which was expected on the ground that LDA has a tendency to overmetallize bonding. The simplified ADSIC (open squares) scheme [38] gives in general rather poor results. Mind that ADSIC nevertheless allows a fair reproduction of bonding properties in poly-acetylene [44]. It obviously fails in the case of the more sensitive polarizability. GSlat (crosses) in turn reproduces very well the exact SIC tendencies, while the standard SIC-Slater (full squares) is completely wrong for intermediate intermolecular distances. This mismatch is correlated to a similar failure of standard SIC-Slater in the potential energy surface at intermediate distances [29]. And both failures can be tracked back to delocalization effects of the orbitals at critical configurations. GSlat allows to keep the wave functions entering the Hamiltonian localized and thus performs much better. We checked that standard SIC-KLI (not shown in the figure) does not cure this mismatch. For large intermolecular distances, standard SIC-Slater and GSlat results come close to each other because there remain two separated H_2 molecules, which have each only one electron in each spin subspace.

3.2 The C_2 dimer and the C_4 chain

Another interesting case is provided by small carbon chains whose electrical excitation properties are well studied [45,46,47]. We consider here two examples, namely the C_2 dimer and the C_4 chain. Since, to the best of our knowledge, there exist no experimental results for the polarizabilities of those systems, our aim is to compare various theoretical approaches using exact SIC as a benchmark. We recall that we already demonstrated the quality of GSlat in the case of a single carbon atom in [29] for exchange only calculations. In exchange correlations calculations, the C atom polarizability is again well reproduced by GSlat. As the electronic cloud in the C atom is slightly axially deformed because of the single occupation of $2p_x$ and $2p_y$ orbitals (while the $2p_z$ orbital is unoccupied), one measures different polarizabilities along the x, y axes and along the z axis. To put the subsequent results on C molecules into perspective, we quote here briefly the polarizations for the C atom : along z axis, $\alpha_z = 10.40 a_0^3$ for both SIC and GSlat, along x, y axes, $\alpha_{x,y} = 11.52 a_0^3$ for GSlat and $11.76 a_0^3$ for SIC.

In Fig. 3, we present the longitudinal and transverse polarizabilities for C_2 and C_4 calculated in various approximations. The calculations of [45,48] yield comparable values. In [45], the longitudinal polarizability for C_2 is $\alpha_{\parallel} = 25 a_0^3$ for the ab initio methods and $34 a_0^3$ for LDA/GGA, while the transverse one is $\alpha_{\perp} = 25 a_0^3$ or $100 a_0^3$ respectively, the latter value being a strange exception. The results for C_4 are $\alpha_{\parallel} = 92$ or $94 a_0^3$ and $\alpha_{\perp} = 30$ or $32 a_0^3$. Our results are

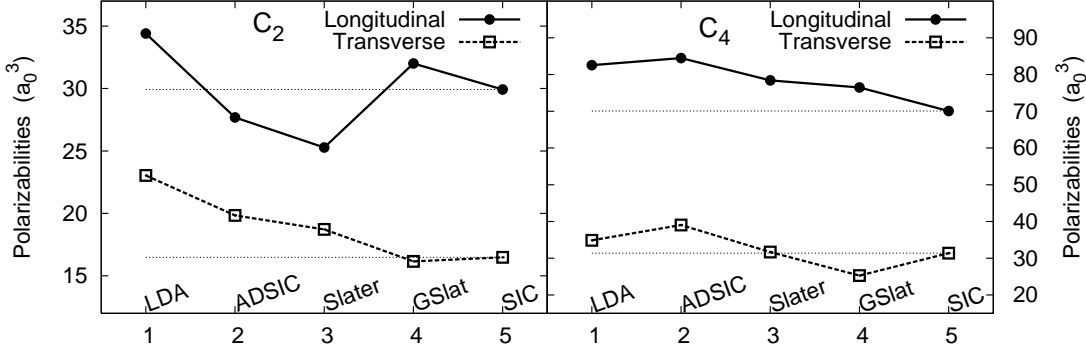


Fig. 3. Transverse and longitudinal polarizabilities of the C_2 molecule (left) and the C_4 chain (right), calculated in various SIC schemes. Horizontal lines emphasize the SIC benchmark values and ease the comparison with the other results.

generally lower for α_{\perp} . It is worth noting that our calculations differ in the employed functionals and pseudopotentials which both can have a sensitive influence on the results. Thus the comparison as a whole looks satisfying. To stay on the safe side, we concentrate on the comparison of approaches within the same setup.

Fig. 3 shows again that GSlat provides a very good approximation to exact SIC in C_2 and much better than any other approximation. The situation is more mixed in the case of C_4 . The values are larger and the relative effects are smaller than for the C_2 dimer. GSlat comes still closest to SIC for the longitudinal mode, but standard SIC-Slater is competitive for the transverse mode. Still, when considering all cases together (C_2 and C_4 , transverse and longitudinal polarizabilities), it is clear that GSlat provides a very good approximation (generally the best one) to the exact SIC.

3.3 Metal clusters

As a final test case, we consider a small sodium cluster representative of simple metallic systems. We have chosen the Na_5 cluster because it has a very soft electron cloud and is thus a most critical test case amongst metallic particles [49]. The cluster is planar (see structure in the insert of Fig. 4) which corresponds to a triaxial shape, and has accordingly different polarizabilities along the three major axes of the system. Fig. 4 shows the polarizabilities of the Na_5 . We obtain much larger absolute values of polarizabilities than in the case of organic systems due to the metallic nature of bonding (delocalization and lower binding). Not surprisingly, LDA performs rather well, for sure better than in organic systems, as is to be expected for a simple metallic system. Even if LDA works very well on those kind of systems, we still see a non negligible difference with the benchmark SIC for the X direction, about 7% for

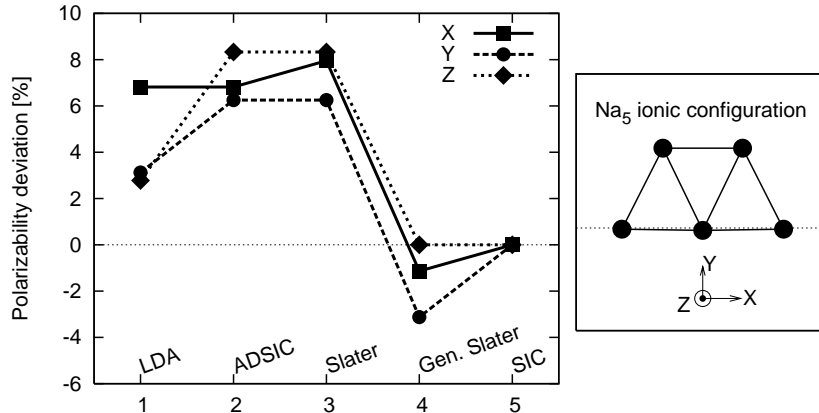


Fig. 4. Polarizabilities of the Na_5 metal cluster (displayed in the right panel), for various SIC schemes as indicated. Horizontal lines emphasize the SIC benchmark values and ease the comparison with the other results.

LDA. Again, GSlat stays closest to the benchmark in all cases.

4 Conclusion

We have tested a newly developed DFT-SIC scheme, called Generalized SIC-Slater (GSlat), with respect to polarizability in chain molecules and a soft metal cluster. GSlat starts from the Optimized Effective Potential (OEP) approach to SIC and handles that in terms of two different sets of N single-particle wave functions. One set is taken for the solution of the OEP equations, thus diagonal in energy and most likely delocalized. The other set is used in setting up the SIC energy which becomes lowest for localized wave functions. Both sets are connected by a unitary transformation which leaves key features as, e.g, the total density invariant. Using that double set allows to accommodate two conflicting demands, energy diagonality versus locality. The unitary transformation is determined by minimization of the SIC energy which leads to what is called the symmetry condition, a key building block of the SIC equations. The localized character of the SIC optimizing set is well suited to justify the steps from OEP to SIC-KLI and further to the SIC-Slater approximation. Thus SIC-OEP with double-set representation and subsequent SIC-Slater approximation leads to the GSlat scheme. By virtue of the double-set technique, it has more flexibility than standard SIC-KLI or SIC-Slater approximation.

As it is known that the polarizability in chain molecules is a sensitive observable for DFT approaches, we have investigated the performance of the new scheme with respect to polarizability in a variety of critical test cases : H chains which mimic the electronic properties of polymers, the C_2 dimer, a C_4 chain, and Na_5 as a soft small metallic particle. The results demonstrate that

the GSlat approximation comes generally close to the values from exact SIC which we use here as a benchmark. It solves the pathologies of the standard SIC-Slater approximation which occur in critical (transitional) molecular configurations such that its performances depend much less on the kind of studied system and configuration (which is not the case in standard SIC-Slater or SIC-KLI). For long H chains, some deviation is observed, which remains reasonable compared to the other schemes and to the less important numerical cost of the GSlat scheme. However addition of the SIC-KLI correction (coming from Generalized SIC-OEP) allows to improve substantially the results. Nevertheless, no strong argument justifies *a priori* the approximate form in Eq. (11), even for spatially symmetrical systems. And the case has yet to be tested for asymmetrical systems. We here checked that GSlat performs fairly good as well in H chains than in less symmetrical systems as C chains or Na clusters. We finally checked that the improvement of the SIC-KLI correction over GSlat is negligible when looking for other observables as energies.

This work was supported, by Agence Nationale de la Recherche (ANR-06-BLAN-0319-02), the Deutsche Forschungsgemeinschaft (RE 322/10-1), and the Humboldt foundation.

References

- [1] W. Kohn, Rev. Mod. Phys. **71** (1999) 1253.
- [2] R G Parr, W Yang, *Density-Functional Theory of Atoms and Molecules*, Oxford University Press, Oxford, 1989.
- [3] R. M. Dreizler, E. K. U. Gross, *Density Functional Theory: An Approach to the Quantum Many-Body Problem*, Springer-Verlag, Berlin, 1990.
- [4] R. O. Jones, O. Gunnarsson, Rev. Mod. Phys. **61** (1989) 689.
- [5] J. P. Perdew, K. Burke, M. Ernzerhof, Phys. Rev. Lett. **77** (1996) 3865.
- [6] M. S. Hybertsen, S. G. Louie, Phys. Rev. B **34** (1986) 5390.
- [7] R. M. Nieminen, Current Opinion in Solid State and Materials Science **4** (1999) 493.
- [8] S. J. A. van Gisbergen, P. R. T. Schipper, O. V. Gritsenko, E. J. Baerends, J. G. Snijders, B. Champagne, B. Kirtman, Phys. Rev. Lett. **83** (1999) 694.
- [9] S. Kümmel, L. Kronik, J. P. Perdew, Phys. Rev. Lett. **93** (2004) 213002.
- [10] J.P. Perdew, Chem. Phys. Lett. **64** (1979) 127.
- [11] J.P. Perdew, A. Zunger, Phys. Rev. B **23** (1981) 5048.
- [12] J. G. Harrison, R. A. Heaton, C. C. Lin, J. Phys. B **16** (1983) 2079.

- [13] S. Goedecker, C.J. Umrigar, Phys. Rev. A **55** (1997) 1765.
- [14] J. Messud, P.M. Dinh, P.-G. Reinhard, E. Suraud, Phys. Rev. Lett. **101** (2008) 096404.
- [15] S. Kümmel, L. Kronik, Rev. Mod. Phys. **80** (2008) 3.
- [16] J.B. Krieger, Y. Li, G. J. Iafrate, Phys. Rev. A **45** (1992) 101.
- [17] J.B. Krieger, Y. Li, G. J. Iafrate, Phys. Rev. A **46** (1992) 5453.
- [18] C. A. Ullrich, U. J. Gossmann, E. K. U. Gross, Phys. Rev. Lett. **74** (1995) 872.
- [19] J. P. Perdew, M. Levy, Phys. Rev. Lett. **51** (1983) 1884.
- [20] M. Mundt, S. Kümmel, Phys. Rev. Lett. **95** (2005) 203004.
- [21] J. B. Krieger, Y. Li, G. J. Iafrate, Phys. Lett. A **146** (1990) 256.
- [22] R. T. Sharp, G. K. Horton, Phys. Rev. **90** (1953) 317.
- [23] T. Körzdörfer, M. Mundt, S. Kümmel, Phys. Rev. Lett. **100** (2008) 133004.
- [24] C. Edmiston, K. Ruedenberg, Rev. Mod. Phys. **35** (1963) 457.
- [25] M. Pederson, R. A. Heaton, C. C. Lin, J. Chem. Phys. **80** (1984) 1972.
- [26] J. Garza, J. A. Nichols, D. A. Dixon, J. Chem. Phys. **112** (2000) 7880.
- [27] S. Patchkovskii, J. Autschbach, T. Ziegler, J. Chem. Phys. **115** (2001) 26.
- [28] C. D. Pemmaraju, S. Sanvito, K. Burke, Phys. Rev. B **77** (2008) 121204.
- [29] J. Messud, P.M. Dinh, P.-G. Reinhard, E. Suraud, Chem. Phys. Lett. **461** (2008) 316.
- [30] J. Messud, P.M. Dinh, P.-G. Reinhard, E. Suraud, Ann. Phys. (N.Y.) **324** (2009) 955.
- [31] T. Körzdörfer, S. Kümmel, M. Mundt, J. Chem. Phys. **129** (2008) 014110.
- [32] J. C. Slater, Phys. Rev. **81** (1951) 385.
- [33] F. Calvayrac, P.-G. Reinhard, E. Suraud, C.A. Ullrich, Phys. Rep. **337** (2000) 493.
- [34] M. Ma, P.-G. Reinhard, and E. Suraud Eur. Phys. J. D **33** (2005) 49.
- [35] Z.P. Wang, P.M. Dinh, P. G. Reinhard, E. Suraud, G. Bruny, C. Montano, S. Feil, S. Eden, H. Abdoul-Carime, B. Farizon, M. Farizon, S. Ouaskit, and T.D. Maerk, Intern. J. Mass Spectr. (2009) in press.
- [36] S. Kümmel, M. Brack, and P.-G. Reinhard, Phys. Rev. B **58** (1998) 1774.
- [37] S. Goedecker, M. Teter, and J Hutter, Phys. Rev. B **54** (1996) 1703.
- [38] C. Legrand, E. Suraud, P.-G. Reinhard, J. Phys. B **35** (2002) 1115.

- [39] O. V. Gritsenko, E. J. Baerends, Phys. Rev. A **64** (2001) 042506.
- [40] C. K. Chiang, C. R. Fincher, Jr., Y. W. Park, A. J. Heeger, H. Shirakawa, E. J. Louis, S. C. Gau, Alan G. MacDiarmid, Phys. Rev. Lett. **39** (1977) 1098.
- [41] S. Kümmel, L. Kronik, J. P. Perdew, Phys. Rev. Lett. **93** (2004) 21.
- [42] B. Champagne, D. H. Mosley, M. Vrakó, and J.-M. André, Phys. Rev. A **52** (1995) 178.
- [43] A. Ruzsinszky, J. P. Perdew, G. I. Csonka, G. E. Scuseria, O. A. Vydrov, Phys. Rev. A **77** (2008) 060502(R).
- [44] I. Ciofini, C. Adamo, H. Chermette, J. Chem. Phys. **123** (2005) 121102.
- [45] M. Bianchetti, P.F. Buonsante, F. Ginelli, H.E. Roman, R.A. Broglia, F. Alasia, Phys. Rep. **357** (2002) 459.
- [46] A. Van Orden, R. J. Saykally, Chem. Rev. **98** (1998) 2313.
- [47] J. D. Watts, R. J. Bartlett, J. Chem. Phys. **97** (1992) 3445.
- [48] A. Abdurahman, A. Shukla, G. Seifert, Phys. Rev. B **66** (2002) 155423.
- [49] M. Mundt, S. Kümmel, R. van Leeuwen, P.-G. Reinhard, Phys. Rev. A **75** (2007) 050501.